

## Transport and thermodynamical properties of $\text{Yb}(\text{Cu},\text{Al})_5$ compounds

To cite this article: E Bauer *et al* 1992 *J. Phys.: Condens. Matter* **4** 7829

View the [article online](#) for updates and enhancements.

### Related content

- [Magnetic and transport properties in  \$\(\text{Ce}, \text{La}\)\text{Cu}\_2\text{Ga}\$ : evolution of the Kondo state](#)  
E Bauer, E Gratz, J Kohlmann *et al*.
- [Magnetic structure and field-dependent properties of  \$\text{CeCu}\_5\$](#)   
E Bauer, M Rotter, L Keller *et al*.
- [Thermal conductivity in  \$\text{Ce}\(\text{Cu},\text{Al}\)\_5\$  compounds](#)  
E Bauer, E Gratz, G Hutflesz *et al*.

### Recent citations

- [Intermediate valence to heavy fermion through a quantum phase transition in  \$\text{Yb}\_3\(\text{Rh}\_1\text{xTx}\)\_4\text{Ge}\_{13}\$  \(T=Co, Ir\) single crystals](#)  
Binod K. Rai *et al*
- [Magnetic and transport properties of selected  \$\text{YbxGd}\_{1-x}\text{Ni}\_5\$  intermetallics](#)  
Anna Bajorek *et al*
- [Temperature dependence of the Yb valence in  \$\text{YbCu}\_{1-x}\text{Al}\_x\$  and  \$\text{YbCu}\_{1-x}\text{Al}\_x\$  Kondo compounds studied by x-ray spectroscopy](#)  
H. Yamaoka *et al*



EEG/ECOG AMPLIFIERS  
& ELECTRODES  
ELECTRICAL/CORTICAL  
STIMULATORS  
REAL-TIME PROCESSING

g.tec

[gtec.at/shop](https://gtec.at/shop)

SHOP NOW

## Transport and thermodynamical properties of $\text{Yb}(\text{Cu}, \text{Al})_5$ compounds

E Bauer†, R Hausert†, E Gratz†, D Gignoux‡, D Schmitt‡ and J Sereni§

† Institut für Experimentalphysik, Technische Universität Wien, A-1040 Wien, Austria

‡ Laboratoire Louis Neel, CNRS Grenoble, F-38042 Grenoble, France

§ Centro Atomico Bariloche, Bariloche, Argentina

Received 4 July 1992

**Abstract.** Substitutions for Cu with Al in  $\text{YbCu}_5$  stabilize the hexagonal  $\text{CaCu}_5$  structure and cause a crossover from a divalent behaviour of the Yb ion in  $\text{YbCu}_5$  to a stable integer 3+ behaviour of Yb in  $\text{YbCu}_3\text{Al}_2$ . Additionally, this substitution is responsible for the appearance of long-range magnetic order of a certain antiferromagnetic type in the compound  $\text{YbCu}_3\text{Al}_2$  below 1.9 K.

### 1. Introduction

Like Ce- and U-based compounds, Yb intermetallics are the subject of extensive studies since a wide variety of physical properties are observable, including intermediate valence and Kondo lattice behaviour. Properties within the latter model are well accounted for considering results of the  $j = 7/2$  Coqblin–Schrieffer Hamiltonian [1]. As a hallmark of theoretical progress, the magnetic susceptibility, the specific heat and the field-dependent magnetization of the compound  $\text{YbCuAl}$  have been described successfully on the basis of spin-compensated  $j = 7/2$  impurities [2].

The series  $\text{YbCu}_x$  has been investigated in detail, leading to at least five intermetallic compounds [3]. Three of them ( $\text{YbCu}$ ,  $\text{YbCu}_2$  and  $\text{YbCu}_5$ ) are characterized by intermediate-valence behaviour while the others ( $\text{Yb}_2\text{Cu}_7$  and  $\text{Yb}_2\text{Cu}_9$ ) show Curie–Weiss behaviour, where the Curie constant indicates a 3+ state of the Yb ions.

Particularly,  $\text{YbCu}_5$  is known to be the basis for a set of compounds which are formed by an exchange of Cu with other non-magnetic elements like Au, Ag, Pd, Al, Ga or In [4–6]. Within these substituted compounds, two subgroups may be distinguished.

(i) Compounds crystallizing in the cubic  $\text{AuBe}_5$  structure. The most interesting compounds within this group are  $\text{YbCu}_4\text{Au}$ ,  $\text{YbCu}_4\text{Ag}$ ,  $\text{YbCu}_4\text{Pd}$  and  $\text{YbCu}_4\text{In}$ . As a result of such substitutions, fully ordered ternary compounds (MgSnCu<sub>4</sub>-type) are formed. Being different from the starting divalent  $\text{YbCu}_5$ , the substituted compounds are driven to the 3+ state of the Yb ion.  $\text{YbCu}_4\text{Au}$  and  $\text{YbCu}_4\text{Pd}$  order magnetically below 1 K, while no magnetic order was found in  $\text{YbCu}_4\text{Ag}$  down to the lowest temperatures [4]. This latter compound exhibits a pronounced Kondo lattice behaviour, with most of the physical properties being described by a characteristic

temperature  $T_0$  of about 150 K [7]. A very unusual temperature-induced valence transition was found in  $\text{YbCu}_4\text{In}$  below  $T_v = 40$  K, where the Yb valence changes from 3 at high temperatures to about 2.8 below  $T_v$  [6].

(ii) Compounds crystallizing in the hexagonal  $\text{CaCu}_5$  structure. When Cu in  $\text{YbCu}_5$  is substituted for with Al or Ga, the hexagonal phase is stabilized [5, 8]. It has been proven that at least two Cu ions can be substituted for with Al without altering the crystal structure. Since the  $\text{CaCu}_5$  phase possesses two inequivalent Cu sites, the compound formed by the substitution is not necessarily an ordered one. An analysis of the x-ray line profile and intensity shows that Al is built into the crystal structure exclusively on the 3g sites [9], similarly to in  $\text{Ce}(\text{Cu}, \text{M})_5$  compounds ( $\text{M} = \text{Al}, \text{Ga}$ ) [10]. However, these ions seem to be distributed statistically on these sites.

The aim of the present paper is to investigate in detail the changes in the physical properties of  $\text{YbCu}_5$  resulting from the substitution for Cu with Al.

## 2. Experimental details

Polycrystalline  $\text{Yb}(\text{Cu}_x\text{Al}_{1-x})_5$  samples ( $0.6 \leq x < 1$ ) were prepared by high-frequency melting in an argon atmosphere and subsequently annealed for 14 days at 700 °C. The phase purity and the lattice parameters have been determined in a standard x-ray diffractometer, using  $\text{Co K}\alpha$  radiation. The deduced lattice parameters (collected in table 1) indicate that the volume of the unit cell increases with increasing Al content. Electrical resistivity data were taken by means of a conventional four-probe technique in the temperature range 1.5–300 K. Bulk magnetization measurements were performed using the extraction method, in magnetic fields up to 8 T and in a temperature range 1.5–300 K; low-field susceptibility was then deduced from Arrott plots. A fully automated Nernst calorimeter was used to measure the temperature-dependent specific heat.

Table 1. Lattice parameters of  $\text{Yb}(\text{Cu}_x\text{Al}_{1-x})_5$ .

$x$	$a$ (Å)	$c$ (Å)	Reference
1.0	4.993	4.126	†
0.9	5.008	4.117	‡
0.8	5.026	4.150	‡
0.6	5.106	4.146	‡

† [3].

‡ This work.

## 3. Results and discussion

The temperature-dependent resistivity  $\rho$  of various  $\text{Yb}(\text{Cu}_x\text{Al}_{1-x})_5$  compounds is shown in figure 1. The variation of  $\rho$  for the selected compounds is found to be strongly temperature dependent, in contrast to the resistivity data results reported for other divalent Yb–Cu compounds [11]. This indicates that the substitution for Cu with Al drives the system from a divalent state and therefore a non-magnetic one in

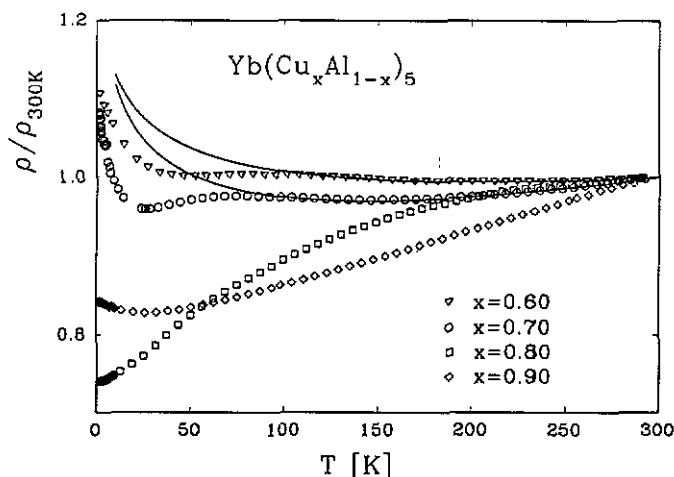


Figure 1. Temperature dependence of the electric resistivity  $\rho$  of various  $\text{Yb}(\text{Cu}_x\text{Al}_{1-x})_5$  compounds plotted in a normalized representation.

$\text{YbCu}_5$  [3] to a magnetic state of the Yb ions in the substituted compounds. This causes additional scattering interactions, raising the absolute resistivity values over the entire temperature range. Interactions between conduction electrons and magnetic moments in the paramagnetic temperature range, which are known to be strongly temperature dependent, are due to crystal-field splitting and Kondo scattering. The behaviour of the latter interaction mechanism was first described by Kondo [12] and is well accounted for by a negative logarithmic temperature dependence. To demonstrate whether such a dependence of the measured data is apparent in the  $x = 0.60$  and  $0.70$  samples, we have analysed the results in the high-temperature range considering the most important scattering mechanisms,

$$\rho(T) = \rho_0 + \rho_{\text{ph}}(T) + \rho_{\text{mag}}(T) = a + bT - c \ln(T) \quad (1)$$

where  $\rho_0$  is due to scattering of conduction electrons on lattice imperfections,  $\rho_{\text{ph}}(T)$  describes the resistivity contribution due to the interaction of conduction electrons with thermally excited phonons, whereas  $\rho_{\text{mag}}(T)$  arises from scattering processes with magnetic moments. At elevated temperatures, the different contributions to  $\rho(T)$  follow simple analytical temperature dependencies (compare equation (1)). A least-squares fit of the experimental data to this equation shows satisfactory agreement and thus proves the importance of the Kondo interaction for these compounds. These fits are shown as full lines in figure 1. Below about 100 K, the experimental data are seen to deviate strongly from the theoretical behaviour considered. These discrepancies are attributed to the acting crystalline electric field, which lifts the eightfold-degenerate ground state of the  $\text{Yb}^{3+}$  ion. The action of the crystal field in hexagonal symmetry ( $\text{CaCu}_5$  structure) splits the  $j = 7/2$  ground state of the Yb ion into four doublets with eigenstates  $j_z = \pm 1/2, \pm 3/2, \pm(\frac{7}{2}\alpha + \frac{5}{2}\beta)$  and  $\pm(\frac{7}{2}\alpha - \frac{5}{2}\beta)$ . The agreement of the fit with the data above  $\approx 100$  K indicates that the magnetic scattering processes happen either in the full  $7/2$  state, or, alternatively, the overall crystal-field splitting  $\Delta_{\text{CEF}}$  is much larger than the room temperature.

To get full information concerning the magnetic contribution to the total electrical resistivity  $\rho(T)$ , it is necessary to eliminate the residual resistivity  $\rho_0(T)$ , as well as the phonon part  $\rho_{\text{ph}}(T)$ . Usually, this is done by comparing the resistivity data of the magnetic compounds with those of the appropriate isostructural non-magnetic compounds. Equivalent non-magnetic compounds are members of the  $\text{La}(\text{Cu}, \text{Al})_5$  series. A comparison with the Lu-based series is more problematic since  $\text{LuCu}_5$  crystallizes in the cubic  $\text{AuBe}_5$  structure and furthermore does not follow the Bloch-Grüneisen behaviour.

Figure 2 shows the temperature-dependent resistivity for some of the equivalent non-magnetic compounds. For the reasons outlined above, we have chosen  $\text{La}(\text{Cu}, \text{Al})_5$  compounds to investigate the electron-phonon contribution in Yb compounds. To emphasize the alteration of the electron-phonon interaction due to the increasing Al content, we have subtracted the residual resistivity. This latter contribution rises considerably with rising Al content; this is caused in part by the decreasing mechanical quality of the samples, and, at least partly, by atomic disorder in the crystallographic unit cell. This disorder arises from a statistical distribution of the Al ions on the 3g sites of the hexagonal  $\text{CaCu}_5$  structure.

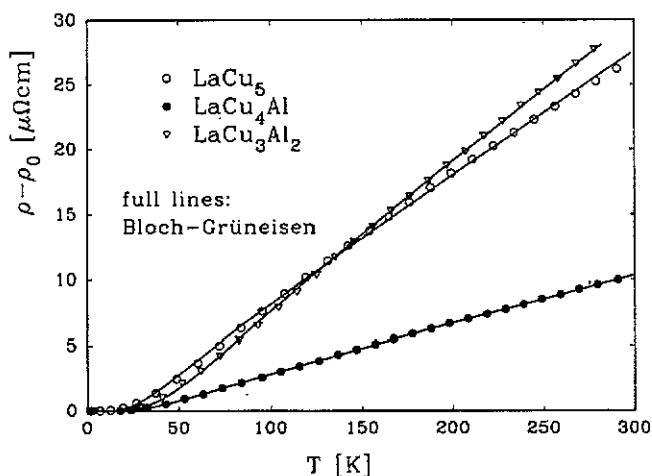
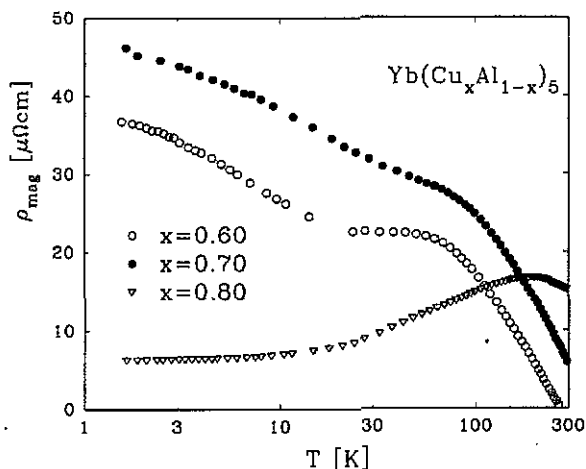


Figure 2. Temperature-dependent electron-phonon contribution to the electric resistivity  $\rho - \rho_0$  of various La compounds. The full lines are fits according to the Bloch-Grüneisen law.

The  $\rho(T)$  behaviour of the  $\text{La}(\text{Cu}, \text{Al})_5$  samples shows the dependence expected of normal metallic compounds and is therefore satisfactorily described within the Bloch-Grüneisen model [13]. This model depends on two adjustable parameters, the temperature-independent electron-phonon interaction constant  $R$  and the Debye temperature  $\theta_D$ . The results of a least-squares fit to the data are shown in figure 2 by full lines. As a result of Al substitution, an evolution of the Debye temperature is found, changing from 160 K for  $\text{LaCu}_5$ , to 202 K for  $\text{LaCu}_4\text{Al}$  and 246 K for  $\text{LaCu}_3\text{Al}_2$ . This indicates that the coupling of the ions strengthens upon this substitution. The electron-phonon interaction constants  $R$  are nearly identical for  $\text{LaCu}_5$  and  $\text{LaCu}_3\text{Al}_2$  ( $R \approx 0.1 \mu\Omega \text{ cm K}^{-1}$ ) but smaller for  $\text{LaCu}_4\text{Al}$  ( $R \approx 0.04 \mu\Omega \text{ cm K}^{-1}$ ). However,

it should be noted that the magnitude of  $R$  depends sensitively on the values of the absolute resistivity which can be influenced by cracks and other mechanical inhomogeneities of the samples.



**Figure 3.** Temperature-dependent magnetic contribution to the electrical resistivity  $\rho_{\text{mag}}$  of various  $\text{Yb}(\text{Cu}_x\text{Al}_{1-x})_5$  compounds plotted in a semilogarithmic representation.

The magnetic contribution to the electrical resistivity  $\rho_{\text{mag}}(T)$  of  $\text{Yb}(\text{Cu}, \text{Al})_5$  compounds is then found by subtracting the resistivity data for the isostructural non-magnetic La-based compounds. Results are shown in figure 3 in a semilogarithmic representation. The accuracy of the  $\rho_{\text{mag}}$  values is constrained by the above-mentioned uncertainties. All the compounds indicated are characterized by ranges with a negative logarithmic resistivity behaviour. This particular behaviour is well known for the Kondo interaction between the conduction electrons and almost localized magnetic moments. However, this simple analytical behaviour is strongly modified when the crystal-field splitting of the magnetic ions becomes important. The electrons can suffer additional scattering interactions with the magnetic moments, caused by the thermal population of the different crystal-field levels. This results in increasing resistivity values. Both mechanisms mentioned have been described successfully by Cornut and Coqblin [14]. They have shown that for temperatures much larger and much smaller than the energy of a certain crystal-field level, a logarithmic behaviour due to Kondo interaction appears, while the temperature of the maximum in  $\rho_{\text{mag}}(T)$  characterizes the energy separation of the crystal-field level from the ground state. However, this clear-cut behaviour is only found in those cases where all the levels are well separated. The ratio  $Q$  of the slopes of the logarithmic ranges reflects the degeneracy of the crystal-field levels involved. Following the model of Cornut and Coqblin [14], the deduced ratio of about 3.95 for both  $x = 0.60$  and  $0.70$  compounds indicates a quartet ground state ( $Q^{\text{theor}} = 4.2$  [14]) rather than the expected doublet ground state ( $Q^{\text{theor}} = 21$  [14]). Since a crystal field with hexagonal symmetry yields just doublets for Kramers ions, it is supposed that the first excited crystal-field level is not well separated from the ground state. It can also be concluded that the four doublets are fully populated in a range between 200 K and 300 K.

Figure 4 exhibits the temperature-dependent magnetic susceptibility  $\chi$  of various  $\text{Yb}(\text{Cu}_x\text{Al}_{1-x})_5$  compounds, plotted as  $\chi^{-1}$  versus  $T$  in the temperature range from 1.5 K to room temperature. Starting with the sample  $x = 0.90$ , which is characterized by strongly temperature-dependent  $\chi^{-1}(T)$ , an evolution towards the Curie-Weiss behaviour for compounds with higher Al content is found. This can be concluded from the linear dependence of  $\chi^{-1}(T)$  in the latter compounds and at temperatures above about 80 K. Deviations from the Curie-Weiss behaviour in these compounds below this temperature range indicate crystal-field effects, which are not expected for intermediate-valence systems.

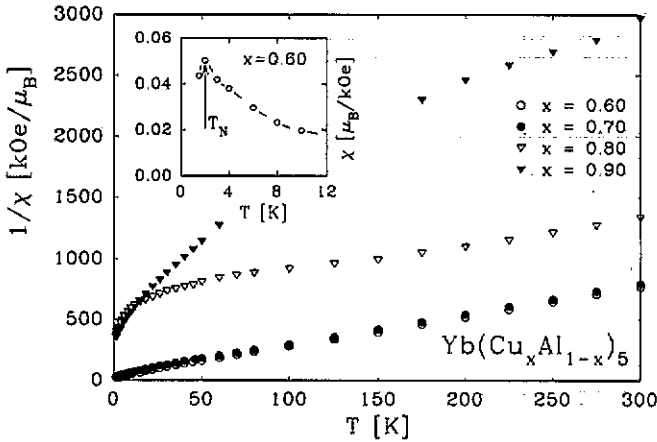


Figure 4. Temperature-dependent magnetic susceptibility  $\chi$  of  $\text{Yb}(\text{Cu}_x\text{Al}_{1-x})_5$  compounds plotted as  $\chi^{-1}$  versus  $T$ . The inset shows the low-temperature susceptibility for  $x = 0.60$ . The arrow indicates the magnetic phase transition.

Analysing the susceptibility data above about 80 K according to

$$\chi = \chi_0 + \frac{C}{T - \theta_p} \quad (2)$$

yields information concerning the temperature-independent Pauli contribution  $\chi_0$ , the effective magnetic moment  $\mu_{\text{eff}}$  (deduced from the Curie constant  $C$ ) and the paramagnetic Curie temperature  $\theta_p$ . The Pauli contribution of the  $\text{Yb}(\text{Cu}_x\text{Al}_{1-x})_5$  compounds investigated steadily decreases with decreasing  $x$  value. This is explained by the Cu 3d contribution 'losing weight' to the electronic density of states. The Curie constant  $C$  hints at a drastic change of the state of the Yb ions in this series, since a crossover from a divalent state reported for  $\text{YbCu}_5$  [3] to a clear 3+ state of Yb in  $\text{YbCu}_3\text{Al}_2$  is found. This latter conclusion can be drawn from the value of the effective magnetic moment of this compound, which is close to the value expected for a free 3+ Yb ion ( $\mu_{\text{eff}}(\text{Yb}^{3+}) = 4.54\mu_B$ ). Simultaneously with the stabilization of the 3+ state, a magnetic phase transition below 1.9 K is found for  $\text{YbCu}_3\text{Al}_2$  (inset in figure 4). The paramagnetic Curie temperature  $\theta_p$  shows a strong concentration dependence, changing from  $-342$  K for  $x = 0.80$  to  $-17.5$  K for  $x = 0.60$ . Very high

values of  $\theta_p$  can be referred to Kondo interaction processes, already deduced from the resistivity behaviour.

The field-dependent magnetization curves of various  $\text{Yb}(\text{Cu}, \text{Al})_5$  compounds are shown in figure 5 for  $T = 1.5$  K. Again, a strong concentration-dependent variation of  $M(H)$  is found. Very small magnetization values are deduced for  $x = 0.90$  and  $x = 0.80$ , and they are nearly linear in their field dependence. The observed dramatic reduction of the magnetic moments shows the predominance of the Kondo effect, related to the unusually large values of  $\theta_p$ . In contrast, the magnetization curves of  $x = 0.70$  and  $0.60$  are characterized by considerably larger values, in agreement with their much weaker paramagnetic Curie temperatures. However, the full saturation moment  $g_J J = 4\mu_B$  cannot be found from the observed  $M(H)$  curves, which indicates the presence of crystal-field splitting. The inset in figure 5 shows  $dM/dH$  versus  $H$  for  $x = 0.60, 0.70$  and  $0.80$ . The  $x = 0.60$  sample exhibits two clear-cut maxima below about 10 kOe, which vanish at temperatures above 2 K. These maxima are attributed to field-induced phase transitions characteristic of some sort of antiferromagnetic order, in agreement with the specific heat and the susceptibility data. For  $x = 0.70$ , both maxima disappear and a change of the slope around 8 kOe is visible instead. Almost no field dependence of  $dM/dH$  is found for  $x = 0.80$  and  $0.90$ .

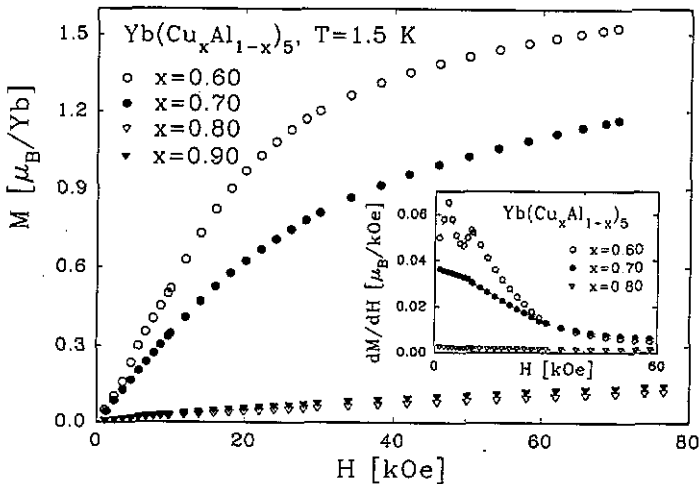


Figure 5. Isothermal magnetization curves ( $T = 1.5$  K) of various  $\text{Yb}(\text{Cu}_x\text{Al}_{1-x})_5$  compounds. The inset shows  $dM/dH$  versus  $H$ .

Specific heat measurements have been performed between 1.45 K and 60 K. Additionally, the compound  $x = 0.70$  has been investigated down to 300 mK. The temperature dependence of the specific heat  $c$  for different compounds, and temperatures below 8 K, is shown in figure 6. The compound with  $x = 0.60$  is characterized by a mean-field-like anomaly, indicating magnetic order below 1.9 K. It is interesting to note that the specific heat peaks at  $4.5 \text{ J}(\text{mol K})^{-1}$  instead of  $12.48 \text{ J}(\text{mol K})^{-1}$  for a conventional magnetic  $s = 1/2$  doublet, which is expected as the ground state of the crystal field in this compound. As we see from the logarithmic ranges of the resistivity data and from susceptibility measurements, the properties of

this compound are mainly determined by the Kondo and RKKY interactions as well as by crystal-field splitting. This causes reduced magnetic moments in the ordered state, corresponding to a phase transition with a reduced specific heat anomaly at the ordering temperature. The magnetic entropy  $S_{\text{mag}}(T)$  for  $x = 0.60$  has been deduced by carefully extrapolating the  $c(T)$  data towards zero and calculating

$$\int c_{\text{mag}}(T) T^{-1} dT$$

where

$$c_{\text{mag}}(T) = (c[\text{Yb}(\text{Cu}_x\text{Al}_{1-x})_5] - c[\text{La}(\text{Cu}_x\text{Al}_{1-x})_5]).$$

The entropy release associated with the phase transition at  $T_N = 1.9\text{K}$  is smaller than that expected for the unperturbed ground-state crystal field ( $= R \ln 2$ ). This either stems from short-range-ordering effects above  $T_N$ , or, as we have mentioned, may reflect the manifestations of the Kondo effect.  $S_{\text{mag}}(T)$  approaches  $5.76\text{J}(\text{molK})^{-1}$  around  $6\text{K}$ , roughly three times the ordering temperature, while  $R \ln 4$  is reached well below  $40\text{K}$ . The crystal-field level diagram thus shows the first excited level near the ground state, in agreement with the conclusions drawn from the resistivity data for this compound.

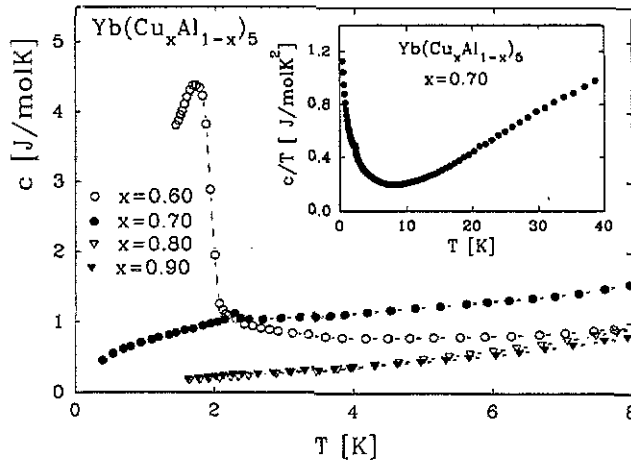


Figure 6. Temperature-dependent specific heat  $c$  of various  $\text{Yb}(\text{Cu}_x\text{Al}_{1-x})_5$  compounds. The inset shows  $c/T$  versus  $T$  for  $x = 0.70$ .

Specific heat results for magnetic Kondo compounds have recently been described very successfully within a molecular-field approach for the  $s = 1/2$  resonant level model [15, 16]. Within this model, the specific heat jump  $\delta c$  at the ordering temperature is calculated numerically as a function of  $T_K/T_N$ . Starting with  $\delta c = 12.48\text{J}(\text{molK})^{-1}$  for a purely magnetic system ( $T_K = 0$ ),  $\delta c$  decreases continuously with increasing  $T_K/T_N$  values, going asymptotically towards zero. Based on this universal behaviour, valid for  $s = 1/2$  systems,  $T_K$  of  $\text{YbCu}_3\text{Al}_2$  can be

deduced using the above-mentioned universal dependence. Thus,  $T_K$  in the ground-state crystal field is estimated to be about 2.6 K. This particular value of  $T_K$  causes the maximum of the Kondo contribution to the specific heat ( $T_{\text{max}}^c \approx 0.45T_K$  [17]) to be covered by the jump in the specific heat associated with the magnetic phase transition at  $T = 1.9$  K. Since the Kondo contribution vanishes steadily above  $T_{\text{max}}^c$ , the observed specific heat of  $\text{YbCu}_3\text{Al}_2$  also decreases above the magnetic ordering temperature.

The sample with  $x = 0.70$  is characterized by a small discontinuity in  $c(T)$  around 2.2 K; this is attributed to impurities in  $\text{Yb}_2\text{O}_3$ , very frequently found in ytterbium compounds (see, e.g., [11]). This oxide is known for an antiferromagnetic phase transition at that temperature. Since the small antiferromagnetic contribution is not resolved in the susceptibility measurements of the same sample, we believe that the overall behaviour of specific heat is not essentially influenced by these magnetic impurities.

The inset in figure 6 displays  $c/T$  versus  $T$  for  $x = 0.70$ . This plot shows a very rapid rise of the electron contribution to the specific heat below about 8 K. This behaviour, which obviously is not connected with the deduced phase transition at 2.2 K, usually characterizes heavy-fermion behaviour, thereby tracing the formation of a strongly temperature-dependent many-body resonance at the Fermi energy. The extra increase in  $c/T$  below 1 K is attributed to a hyperfine contribution, which arises, at least partly, from the quadrupolar splitting of the  $^{173}\text{Yb}$  nuclei and from a possible contribution of  $^{63}\text{Cu}$  and  $^{65}\text{Cu}$  [18].

Representing the temperature-dependent specific heat as  $c/T$  versus  $T^2$  allows us to deduce  $\gamma^{\text{HT}}$  by extrapolating the data from the temperature range  $10 \text{ K} < T < 20 \text{ K}$  towards zero. This procedure shows an increase of  $\gamma^{\text{HT}}$  with rising Al content, starting with  $40 \text{ mJ mol}^{-1}\text{K}^{-2}$  for  $x = 0.90$  and peaking at  $120 \text{ mJ mol}^{-1}\text{K}^{-2}$  for  $x = 0.70$ . The sample with  $x = 0.60$ , in contrast, has a smaller value of  $\gamma^{\text{HT}}$ , which is obviously related to the formation of long-range magnetic order.

#### 4. Summary

A survey of experimental data which has been presented for the series  $\text{Yb}(\text{Cu}_x\text{Al}_{1-x})_5$  clearly indicates that the substitution for Cu with Al drives the compounds at ordinary temperatures to a stable 3+ state of Yb ions.

The deduced transport properties of this series of experiments indicate a Kondo interaction in the presence of crystal-field splitting which becomes more pronounced at higher Al content. The most likely explanation of the observed magnetic contribution to the electric resistivity is a strongly varying overall crystal-field splitting, which decreases with increasing Al content. This is concluded from the temperature-dependent decrease of the maximum in  $\rho_{\text{mag}}(T)$ . The usual Kondo lattice behaviour of the electrical resistivity, i.e. a  $T^2$  law at low temperatures, followed by a well-pronounced maximum, is not obtained from the measurements. It is thought to be prevented by the chemical disorder of the Al and Cu ions on the 3g sites of the crystal, though the Yb ions build up a regular sublattice in the compound.

In the scope of single-ion Kondo models [19], the absolute value of the paramagnetic Curie temperature  $\theta_p$  is closely related to the Kondo temperature  $T_K$  of the system. Since the observed values of  $\theta_p$  of the  $\text{Yb}(\text{Cu}, \text{Al})_5$  compounds investigated are strongly concentration dependent, a sharp drop in  $T_K$  with rising Al

content is inferred. The extremely large values of  $\theta_p$  for  $x \geq 0.80$  are thought to arise from the strong interaction energy of the Kondo process, which causes long-range magnetic order to be suppressed. On the other hand,  $\theta_p$  of  $\text{YbCu}_3\text{Al}_2$  is small ( $-17\text{K}$ ), leading to the possibility that the energy of the Kondo process (responsible for the screening of the magnetic moments) is exceeded by the RKKY interaction which mediates the long-range magnetic order.

### Acknowledgments

Parts of this work have been supported by the Austrian Science Foundation, project P 7608-TEC. One of us (EB) is indebted to the 'Österreichische Forschungsgemeinschaft' for financial support.

### References

- [1] Coqblin B and Schrieffer B 1969 *Phys. Rev.* **185** 3333
- [2] Hewson A C, Newns D M, Rasul J W and Read N 1985 *J. Magn. Magn. Mater.* **47-48** 354
- [3] Iandelli A and Palenzona A 1971 *J. Less-Common Met.* **25** 333
- [4] Rossel C, Yang K N, Maple M B, Fisk Z, Zirngiebl E and Thompson J D 1987 *Phys. Rev.* **35** 1914
- [5] Adroja D T, Malik S K, Padalia B D and Vijayaraghavan R 1987 *J. Phys. C: Solid State Phys.* **20** L30
- [6] Felner I, Nowik I, Vaknin D, Potzel U, Moser J, Kalvius G M, Wortmann G, Schmiester G, Hilscher G, Gratz E, Schmitzer C, Pillmayr N, Prasad K G, deWaard H and Pinto H 1987 *Phys. Rev. B* **35** 6956
- [7] Besnus M J, Haen P, Hamdaoui N, Herr A and Meyer A 1990 *Physica B* **163** 571
- [8] Bauer E, Payer K, Hauser R, Gratz E, Gignoux D, Schmitt D, Pillmayr N and Schaudy G 1992 *J. Magn. Magn. Mater.* **104-107** 651
- [9] Gratz E, Lindbaum A, Rotter M, Bauer E, Mueller H and Kirchmayr H 1992 *Proc. European Powder Diffraction Conf. (Enschede, The Netherlands, 1992)*
- [10] Kim S M, Buyers W J L, Lin H and Bauer E 1991 *Z. Phys. B* **84** 201
- [11] Jaccard D, Junod A and Sierro J 1980 *Helv. Phys. Acta* **53** 583
- [12] Kondo J 1964 *Prog. Theor. Phys.* **32** 37
- [13] Ziman J M 1960 *Electrons and Phonons* (Oxford: Clarendon)
- [14] Cornut D and Coqblin D 1972 *Phys. Rev. B* **5** 4541
- [15] Braghta A 1989 *PhD Thesis* University of Strasbourg
- [16] Besnus M J, Braghta A, Hamdaoui N and Meyer A 1992 *J. Magn. Magn. Mater.* **104-107** 1385
- [17] Desgranges H U and Schotte K D 1982 *Phys. Lett.* **91A** 240
- [18] Amato A, Fisher R A, Phillips N E, Jaccard D and Walker E 1990 *Physica* **165-166** 425
- [19] Gruener G and Zawadowski A 1978 *Progress in Low Temperature Physics* vol VII B ed D F Brewer (Amsterdam: North-Holland) ch 8